Climate change impact on the water regime of two great Arctic rivers: modeling and uncertainty issues

Alexander Gelfan, David Gustafsson, Yury Motovilov, Berit Arheimer, Andrey Kalugin, Inna Krylenko & Alexander Lavrenov

Climatic Change
An Interdisciplinary, International Journal Devoted to the Description, Causes and Implications of Climatic Change

ISSN 0165-0009
Volume 141
Number 3

Climatic Change (2017) 141:499-515
DOI 10.1007/s10584-016-1710-5

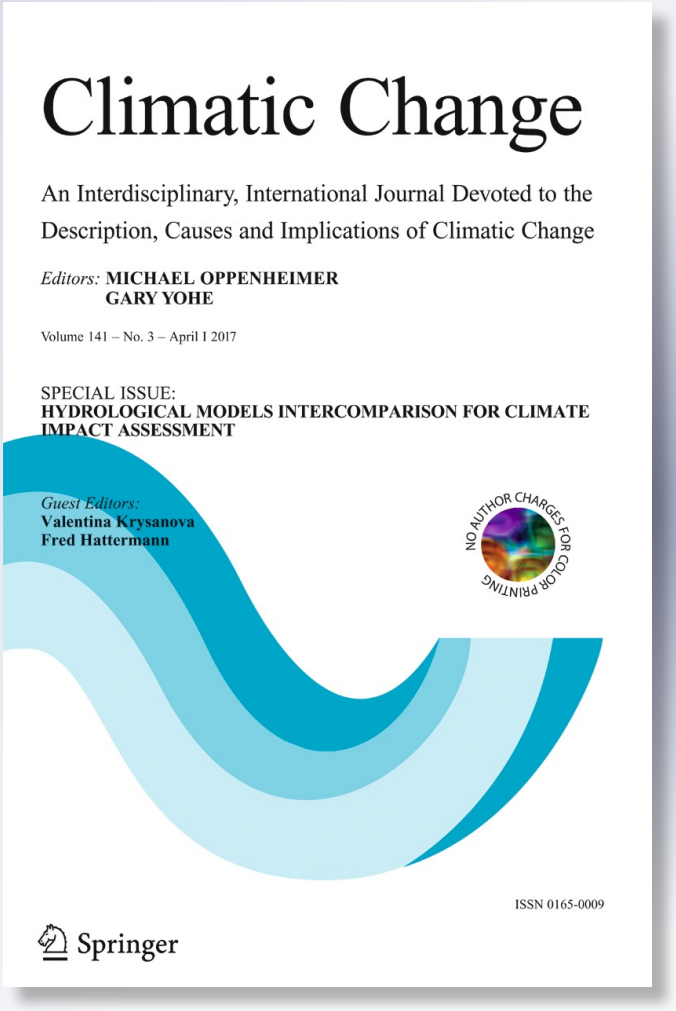

Springer

Climatic Change (2017) 141:499–515
DOI 10.1007/s10584-016-1710-5

Climate change impact on the water regime of two great Arctic rivers: modeling and uncertainty issues

Alexander Gelfan[1,2] · **David Gustafsson**[3] · **Yury Motovilov**[1,2] · **Berit Arheimer**[3] · **Andrey Kalugin**[1,2] · **Inna Krylenko**[1,4] · **Alexander Lavrenov**[1]

Received: 30 November 2015 / Accepted: 20 May 2016 / Published online: 1 June 2016

Abstract The ECOlogical Model for Applied Geophysics (ECOMAG) and the HYdrological Predictions for the Environment (HYPE) process-based hydrological models were set up to assess possible impacts of climate change on the hydrological regime of two pan-Arctic great drainage basins of the Lena and the Mackenzie Rivers. We firstly assessed the reliability of the hydrological models to reproduce the historical streamflow series and analyzed the hydrological projections driven by the climate change scenarios. The impacts were assessed for three 30-year periods (early- (2006–2035), mid- (2036–2065), and end-century (2070–2099)) using an ensemble of five global climate models (GCMs) and four Representative Concentration Pathway (RCP) scenarios. Results show, particularly, that the basins react with a multi-year delay to changes in RCP2.6, so-called "mitigation" scenario, and consequently to the potential mitigation measures. Then, we assessed the hydrological projections' variability, which is caused by the GCM's and RCP's uncertainties, and found that the variability rises with the time horizon of the projection, and generally, the projection variability is larger for the Mackenzie than for the Lena. We finally compared the mean annual runoff anomalies projected under the GCM-based data for the twenty-first century with the corresponding

This article is part of a Special Issue on "Hydrological Model Intercomparison for Climate Impact Assessment" edited by Valentina Krysanova and Fred Hattermann

Electronic supplementary material The online version of this article (doi:10.1007/s10584-016-1710-5) contains supplementary material, which is available to authorized users.

✉ Alexander Gelfan
hydrowpi@mail.ru

[1] Water Problems Institute of RAS, Moscow, Russia

[2] P.P. Shirshov Institute of Oceanology of RAS, Moscow, Russia

[3] Swedish Meteorological and Hydrological Institute, Norrköping, Sweden

[4] Lomonosov Moscow State University, Faculty of Geography, Moscow, Russia

anomalies projected under a modified observed climatology using the delta-change method in the Lena basin. We found that the compared projections are closely correlated for the early-century period. Thus, for the Lena basin, the modified observed climatology can be used as driving force for hydrological model-based projections and considered as an alternative to the GCM-based scenarios.

1 Introduction

To date, approaches for assessing hydrological consequences of climate change at the basin scale are based, increasingly, on numerical experiments, in which regional hydrological models are forced with constructed scenarios of future climate. These scenarios can be either derived by transforming available historical series of meteorological observations or can be simulated by climate models (see reviews in Chiew et al. 2009; Peel and Blöschl 2011; Gelfan et al. 2015a, and references herein). The latter approach provides wide opportunities for analyzing mechanisms of hydrological system responses to climate and assessing physically meaningful changes of the system. Implementation of such opportunities is among key problems in catchment hydrology (see Ehret et al. 2014, among others).

Use of data from global climate models (GCMs) as inputs into regional hydrological models has been ineffective for a long time. This relates mainly to two factors: (1) inconsistency between space and time resolution of GCMs and characteristic scales of hydrological processes in a river basin and (2) inaccuracy in reproducing the observed meteorological characteristics, especially precipitation, at the regional scale (e.g., Kundzewicz and Stakhiv 2010). However, deepening knowledge on climate system component dynamics and developing numerical methods of climate simulation, upgrading measuring technologies and increase in computing resources have resulted in increased predictive skill of GCMs and better agreement between GCMs and regional hydrological models' resolutions in the last decade (Flato et al. 2013). However, inaccuracy in the reproduced historical climate data remains too large for many regions, and these data should be used with precaution for climate change impact studies at the basin scale. In fact, if a hydrological model driven by GCM-produced output does not perform adequately under the historical conditions, then it is reasonable to assume that the model inadequacy is propagated (and probably amplified) in the future (e.g., Knutti 2010).

Even if the GCM-driven hydrological model reproduces historical hydrological data well, the hydrological projections for the future are uncertain. The uncertainty is, primarily, caused by uncertainty in the future climate projections, rather than by the hydrological modeling (e.g., Seiller and Anctil 2014). Climate projection's uncertainty sources can be grouped into three factors (Hawkins and Sutton 2009): (1) climate model structural uncertainty, (2) scenario variability, and (3) natural variability of climate system (so-called "climatic noise"). The scenario and the model structure uncertainties are dominant sources of uncertainty at the regional spatial scale for time horizons of several decades, whereas importance of the climatic noise increases in shorter spatial-temporal scales (Hawkins and Sutton 2009).

Within the Inter-Sectoral Impact Model Intercomparison Project, phase 2 (ISI-MIP2), regional hydrological models forced by GCMs have been applied for simulating hydrological responses under the current and future climate conditions. In this study, we investigate the hydrological regime of two pan-Arctic great basins of the Lena and the Mackenzie Rivers. Two regional hydrological models, namely, ECOlogical Model for Applied Geophysics

(ECOMAG) and Hydrological Predictions for the Environment (HYPE), were set up and applied, while future hydrological projections were driven by the most recent World Climate Research Programme Coupled Model Intercomparison Project phase 5 (CMIP5) GCMs' data.

There are several published studies analyzing the climate impact on the Lena and the Mackenzie basins. The latter basin has been a research subject of many climate and hydrology projects, including the Mackenzie GEWEX Study (MAGS) (Woo et al. 2008). Visible runoff changes in the recent decades were detected in available streamflow records for both the Lena (e.g., Yang et al. 2002; Ye et al. 2003; Berezovskaya et al. 2005) and Mackenzie River (Aziz and Burn 2006; Yip et al. 2012; Yang et al. 2015). Particularly, an increasing trend in annual runoff has been detected along the Lena River basin in recent decades (Berezovskaya et al. 2005). It has been found that warmer temperatures over a winter season caused an increase of seasonal runoff, an advance of snowmelt season from June to late May, and resulted in a lower daily maximum discharge in June (Yang et al. 2002). The Mackenzie River water regime has also changed over the past four decades due to climate variation, with a decrease in maximum spring flow, rise of the cold season baseflow, and weak decreasing trends in the early summer, late fall, and annual mean flow (Aziz and Burn 2006; Yang et al. 2015).

Hydrological projections of climate change for both basins have been developed by Mokhov et al. (2003) and Nohara et al. (2006) on the basis of GCMs. For instance, the multi-GCM ensemble simulations project 16 and 24 % increase in annual runoff in the Lena and Mackenzie basins, respectively, by the end of twenty-first century (Nohara et al. 2006). Similar anomalies for the Lena River are estimated by Mokhov et al. (2003).

Applicability of the GCM-driven hydrological models for climate impact studies has also been reported for these basins (e.g., the global VIC model in Nijssen et al. (2001) and the regional ECOMAG model in Gelfan et al. (2015a)).

In this study, we aim to (1) test an ability of the GCM-driven regional hydrological models for historical runoff simulation in the Lena and Mackenzie River basins, (2) project the hydrological response to climate projections using an ensemble of GCMs and Representative Concentration Pathway (RCP) scenarios, (3) assess the response variability caused by the model (GCM) and scenario (RCP) uncertainties, and (4) compare the hydrological projections driven by the GCM scenario ensemble with the projections forced by a modified observed climatology (delta-change method).

2 Study basins

The Lena Basin ranks ninth in the world in size with a catchment area of 2,460,000 km^2 extending from 103°E to 142°E and from 52°N to 74°N (Fig. A in the supplementary material). The river flows northward from mid-latitudes to the Arctic Ocean (Laptev Sea) and contributes about 15 % of total freshwater flow into the Arctic Ocean (Yang et al. 2002).

The Mackenzie River with a catchment area of 1,800,000 km^2 is the largest river flowing into the Arctic Ocean (Beaufort Sea) from North America and is one of the 10 longest rivers in the world. The basin extends from 102°W to 142°W and from 52°N to 69°N (Fig. A in the supplementary material).

Both basins are located in the zones of continental moderate and subarctic climates. Main types of landscapes are tundra, forest tundra, and forests (taiga). The entire Lena River basin and the most part of the Mackenzie River basin are under the influence of permafrost.

The runoff in the Lena River is characterized by spring snowmelt flood, summer and autumn rain floods, and extremely low water levels in winter. According to the Global Runoff Data Center, mean annual runoff is about 490 km^3 with average annual discharge of about 15,370 m^3/s. Maximum discharge of 189,000 m^3/s was determined at the outlet gauge station Stolb on June 1, 1984.

The hydrological regime of the Mackenzie River is affected by several big lakes influencing runoff regime. The typical hydrograph of the river is characterized by the long snowmelt and the rainfall-driven spring-summer floods. According to the Water Survey of Canada, maximum discharge of 35,000 m^3/s was observed at the outlet gauge Arctic Red River station on May 31, 1992. The average annual discharge of the Mackenzie River is about 10,300 m^3/s.

3 Hydrological models and the basins' data

The process-based semi-distributed regional hydrological models ECOMAG (Motovilov et al. 1999) and HYPE (Lindström et al. 2010) have been applied earlier for hydrological simulations in many river basins of different scales (from tens to millions square kilometers) and located in different hydroclimatic conditions (Motovilov et al. 1999; Gelfan et al. 2015a, b; Arheimer et al. 2012; Donnelly et al. 2015; Pechlivanidis and Arheimer 2015). Both models describe interception of rainfall/snowfall by the canopy, processes of snow accumulation and melt, seasonal freezing and thawing of soil, water infiltration into unfrozen and frozen soil and evaporation from an unfrozen soil layer (so-called, "active layer"), dynamics of soil water content, water routing along a river network, and over and under catchment slopes.

In the ECOMAG model, channel, overland, and subsurface flows are described by the integrated kinematic wave equations (Motovilov et al. 1999). In the HYPE model, water storage appears in various landscape compartments, and different equations regulate the routing and discharge (see detailed description at http://hype.sourceforge.net/). Most of the parameters are physically meaningful and can be assigned from literature or derived through available measured characteristics of topography, soil, and landscape. Some key parameters of the models (e.g., saturated hydraulic conductivity of soil, degree-day factor for snowmelt, field capacity of soil) should be calibrated against streamflow measurements and, if available, measurements of the internal basin parameters and variables (snow characteristics, soil moisture, groundwater level, etc.).

The ECOMAG model is forced by daily precipitation, mean daily values of air temperature, and humidity deficit. Input meteorological variables for the HYPE are daily precipitation and mean daily temperature. Maximum and minimum daily temperatures as well as air humidity and solar radiation can be optionally used by the HYPE model.

The basins' discretization was performed on the basis of global (1-km resolution) DEM data from the HYDRO1K database of the U.S. Geological Survey. To derive soil properties, data of the global HSWD database of land surface parameters at 1-km resolution were used (Fischer et al. 2008). Land use distribution was obtained from the Global Land Cover (GLC) 2000 maps created by the EC Joint Research Centre (Bartholomé and Belward 2005). More detailed digital landscape maps created by the V.V. Dokuchaev Soil Science Institute (1-km resolution) were taken, in addition to the

GLC data, for the ECOMAG model application in the Lena River basin. Input data for the HYPE model can be found at http://hypeweb.smhi.se.

4 Methods

To achieve the above four study objectives, as declared in Sect. 1, four numerical experiments were designed as follows.

4.1 Historical runs of hydrological models driven by WATCH and GCM datasets

Firstly, the hydrological models were evaluated for the present climate conditions. The WATCH reanalysis data, which are based on climate reanalysis data, plus a spatial interpolation (from 1° to 0.5°), elevation correction, and monthly correction based on gridded observations, were used as the models' forcing data for the historical period (1971–2001). The performance of the models was evaluated in terms of daily streamflow data observed at the basins' outlet gauges (Lena—Stolb, Mackenzie—Arctic Red River), provided by the Global Runoff Data Center and Water Survey of Canada. The hydrological models were further driven by the bias-corrected (to WATCH) climate data from five GCMs (GFDL-ESM2M, HadGEM2-ES, IPSL-CM5A-LR, MIROC-ESM-CHEM, and NorESM1-M) for 1971–2005, allowing a comparison of GCM-forced simulations with available observations.

4.2 Assessing the hydrological response to climate projections using an ensemble of GCM and RCP scenarios

Hydrological projections in the study basins were carried out with the help of the hydrological models driven by climate scenarios for the following three 30-year periods: early- (2006–2035), mid- (2036–2065), and end-century (2070–2099). (Note that the first 10 years (2006–2015) are included in order to make all periods of the same length.) As the drivers, we used 20 projections related to all possible combinations of 5 GCMs with 4 RCP scenarios. Mean annual runoff was calculated from the hydrograph projections simulated under each of 20 GCM-RCP-based climate scenarios for each of 3 periods and compared with the mean annual runoff simulated under the corresponding GCM outputs for the reference (historical) period. Thus, 20 annual runoff anomalies were estimated as percentages of the future runoff to the historical one.

Then, we analyzed differences in hydrological responses of both basins to the specific behavior of the four RCP scenarios, which reflect radiative forcing target levels for 2100. According to the overview presented by van Vuuren et al. (2011), they include one mitigation scenario (RCP2.6), two medium stabilization scenarios (RCP4.5 and RCP6.0), and one very high baseline emission scenario (RCP8.5). The first scenario is known also as RCP3 peak-decline scenario, a name that emphasizes the forcing trajectory, first going to the peak forcing level of 3 W/m^2 by 2030–2040 followed by a decline to 2.6 W/m^2 by 2100. The RCP4.5 and RCP6.0 scenarios presume stabilization of the radiative forcing at the corresponding levels (4.5 and 6.0 W/m^2, respectively) around 2100. The RCP8.5 scenario leads to rising radiative forcing to 8.5 W/m^2 by 2100.

In order to compare the obtained hydrological projection trajectories with the specified peculiarities of the four RCP trajectories, we applied the following procedure. First, we

smoothed the simulated annual runoff anomaly time series by the moving average technique with a 30-year sliding window. The technique was applied for 20 (5 GCMs × 4 RCPs) 94-year series (2006–2099) of runoff anomaly simulated by each model for the basins under consideration. The smoothed time series related to the same RCP scenario (but to different GCMs) were averaged, and as a result, we have obtained the smoothed time series of the annual anomalies reflecting the basin hydrological responses to the specific RCP scenario averaged for different GCMs.

4.3 Assessing the hydrological response variability caused by the model (GCM) and scenario (RCP) uncertainties

To quantify contribution of the model (GCM) and scenario (RCP) uncertainties into the variability of runoff projections, we analyzed the following runoff anomalies as hydrological indicators of the basin behavior: long-term mean annual runoff anomaly (MAR anomaly hereafter) and long-term mean monthly runoff anomaly (MMR anomaly hereafter). Twenty values (5 GCMs × 4 RCPs) of the MAR anomaly and 20 × 12 values of the MMR anomaly were calculated for every 30-year period. From these values, mean (M) and standard deviation (SD) were estimated. The interval ($M \pm 1.96$ SD) was assumed as the index of hydrological uncertainty caused by the climate model (GCM) and the scenario (RCP) uncertainties in the climate projections. (Note that in the case of the Gaussian distribution and independence of the projected anomalies, the above formula detects 95 % confidence probability of the interval.) The assigned here interpretation of variability estimate as an indicator of uncertainty is usual within the sampling-based strategy of the uncertainty assessment (see, e.g., review of Pechlivanidis et al. 2011).

4.4 Comparing the hydrological projections driven by the GCM scenario ensemble with the projections forced by the modified observed climatology

Use of the modified observed records as driving forces for hydrological model-based projections is considered as an alternative to the GCM-based scenarios if the latter are uncertain. In hydrological impact studies, this approach is termed as the "delta-change approach" (see, e.g., Xu et al. 2005; Chiew et al. 2009; Peel and Blöschl 2011; Teutschbein et al. 2011). In order to stress source of driving forces, we apply the term "modified observed climatology" (MOC) hereafter. The main advantage of the MOC approach is its simplicity; in its simplest version, only differences between present and future climates (i.e., between the long-term means of the climatic variables) are considered as MOC factors. Disadvantage is, for instance, that the MOC approach considers changes in mean values only, while higher statistical moments (variance, covariation, etc.) of the historical series are assumed to stay unchanged in the future (some other drawbacks of this approach are discussed in details by Xu et al. 2005).

In this study, the MOC factors for the daily historical series (1971–2001) of climate parameters (precipitation, air temperature, and air humidity) were calculated from the GCM-based scenarios for the Lena basin. More specifically, the MOC procedure was designed as follows: first, the basin-averaged mean annual values of climate parameters were determined from the 30-year climate projections simulated by the specific GCM under the specific RCP scenario. Then, these values were compared with the corresponding GCM-simulated values for historical period. As a result of the comparison, 20 (5 GCMs × 4 RCPs) anomalies of the climate parameters with respect to the corresponding simulated parameters of the reference

(historical) period were obtained for each 30-year future period. The obtained anomalies (the MOC factors) were added (for air temperature) and multiplied (for precipitation and air humidity deficit) to the corresponding historical daily series of climate parameters. The modified historical data were used as inputs into the hydrological models. Finally, for each 30-year period, 20 runoff anomalies simulated under the delta-changed historical time series were compared with 20 runoff anomalies simulated under the corresponding GCM data with the same mean.

5 Results and discussion

5.1 Historical runs of hydrological models driven by WATCH and GCM datasets

In Table 1, percent bias (PBIAS) and Nash and Sutcliffe efficiency (NSE) criteria estimated using the observed hydrographs and the hydrographs simulated by the WATCH-driven models are presented. (NSE can range from $-\infty$ to 1; NSE = 1 corresponds to a perfect match of the simulated discharge to the observed data, while NSE $\leq$ 0 indicates that the model predictions are as accurate (or less accurate) as the mean of the observed data.) One can see that both models demonstrate good performance with respect to both criteria. However, the models mostly overestimate runoff, probably because of some bias in the input WATCH data. The detail results of the overall performance of all ISI-MIP2 models, including the ECOMAG and HYPE, for 12 basins, including the Lena and Mackenzie, in terms of monthly discharge, seasonal dynamics, flow duration curves, and extremes are presented by Huang et al. (2016). In brief, both our hydrological models reproduce adequately the monthly discharge, seasonal dynamics, and high flow in both basins; however, the performance in terms of low flow is lower. However, we have to note a large uncertainty in low-flow measurements, especially during cold seasons. For the Lena River, for instance, the long-term mean error of winter daily

Table 1 Performance of the hydrological models: results of evaluation against the observed daily discharge

Forcing	ECOMAG				HYPE			
	Percent bias, %		Nash and Sutcliffe efficiency		Percent bias, %		Nash and Sutcliffe efficiency	
	Lena	Mackenzie	Lena	Mackenzie	Lena	Mackenzie	Lena	Mackenzie
WATCH-reanalysis data								
WATCH	4/7[a]	2.2/−3.5	0.87/0.79	0.88/0.87	7/15	−0.81/5.1	0.97/0.93	0.84/0.89
GCM-output data								
GFDL-ESM2M	12	15	0.67	0.63	5	4.8	0.77	0.7
HadGEM2-ES	9	2	0.54	0.73	9	2.7	0.68	0.67
IPSL-CM5A-LR	7	5.2	0.55	0.62	6	−1.3	0.71	0.65
MIROC-ESM-CHEM	15	13	0.55	0.6	12	0.6	0.68	0.67
NorESM1-M	13	2.7	0.58	0.71	12	−1.1	0.65	0.66
Mean	11.20	7.58	0.58	0.66	8.80	1.14	0.70	0.67

[a] Calibration/validation periods (1971–1986)/(1987–2001)

discharge data is almost 30 %, i.e., four to five times larger than the corresponding error in summer discharge data (Shiklomanov et al. 2006).

The hydrological models were further driven by GCM data for 1971–2001, allowing a comparison of results with the available observations. As expected, the model performance in terms of PBIAS and NSE criteria was reduced in comparison to the WATCH-driven simulations, since the models were "trained" to represent responses for the WATCH data (Table 1). Despite the bias correction of the GCM data against WATCH, bias in hydrological output simulated on the basis of these data still remains. In addition, different GCM-driven hydrological outputs lead to distinguishable results; e.g., PBIAS significantly differs for the Lena River simulations and even more for the Mackenzie River.

The obtained satisfactory simulation results for the historical period provide a basis for the following hydrological model-based climate change impact assessment for both basins.

5.2 Future runs from the GCM projections: assessing hydrological responses and their variability

Mean annual runoff anomalies estimated as percentages of the future runoff (simulated under 20 GCM-RCP combinations of climate scenarios) to the historical runoff (simulated under the corresponding GCM outputs for the reference 1971–2001 period) are presented in Table 2. The anomalies are shown for the following three 30-year periods: early- (2006–2035), mid- (2036–2065), and end-century (2070–2099).

It can be seen from Table 2 that both hydrological models give positive runoff anomalies for almost all GCM-RCP combinations of climate scenarios and for all 30-year periods. Small negative anomalies are obtained only for simulations under some IPSL-CM5A-based scenarios for the Mackenzie basin and can be explained by more significant increase of the projected evaporation modeled under these scenarios. Instead of the several negative anomalies, mean anomalies, obtained by averaging runoff simulations under five GCM-based projections, are positive for all RCP scenarios during twenty-first century. The HYPE-projected anomalies turned out to be more sensitive to the differences in the scenarios. For the Mackenzie basin, mid- and end-century anomalies derived from the HYPE are several percent larger compared to the ECOMAG anomalies. For the Lena basin, otherwise, the ECOMAG-projected anomalies are larger for the early-century period.

A comparison of the obtained hydrological projection trajectories with the specified peculiarities of the four RCP trajectories described above (Sect. 4.2) is shown in Figs. 1 and 2. One can see from these figures that the hydrological models give quite similar runoff trajectories under the same RCP scenario. However, the absolute values of runoff anomalies are slightly different for the ECOMAG and the HYPE models. Importantly, the Mackenzie River runoff anomalies forced with the mitigation RCP2.6 scenario have the same peak-and-decline trajectory as the radiative forcing trajectory; positive runoff anomalies increase and reach maximum in 2040–2069, and then, the anomalies gradually reduce by 2100. According to the RCP2.6 scenario, the radiative forcing peak is projected in 2030–2040 (van Vuuren et al. 2011); i.e., the runoff anomaly peak is projected one to two decades later in the Mackenzie basin. On the other hand, the Lena runoff anomalies simulated under the RCP2.6 scenario stabilize by the last quarter of the century; i.e., they do not demonstrate the peak-and-decline behavior.

To explain the detected features of the runoff trajectories, we analyzed precipitation and temperature projections corresponding to the different RCP scenarios. Figures B and C in the

Table 2 Mean annual runoff anomalies (%) projected under the used GCM and RCP scenarios

Scenario/GCM	RCP2.6			RCP4.5			RCP6.0			RCP8.5		
	2006–2035	2036–2065	2070–2099	2006–2035	2036–2065	2070–2099	2006–2035	2036–2065	2070–2099	2006–2035	2036–2065	2070–2099
ECOMAG-based projections												
Lena River basin												
GFDL-ESM2M	12.8	12.3	21.9	10.4	16.6	21.4	10.8	12.3	19.2	9.4	15.6	23.5
HadGEM2-ES	10.4	17.6	17.2	10.4	19.6	26.2	9.4	17.8	22.7	15.3	18.0	29.5
IPSL-CM5A-LR	14.6	16.6	24.0	15.8	18.2	21.2	13.8	14.0	22.0	13.1	18.7	28.5
MIROC-ESM-CHEM	9.2	15.7	14.0	6.1	14.8	21.7	5.7	17.4	24.7	10.5	20.6	29.7
NorESM1-M	5.7	10.4	17.8	9.7	9.7	22.3	5.4	7.2	13.9	5.2	13.0	18.8
Mean	10.5	14.5	19.0	10.5	15.8	22.6	9.0	13.7	20.5	10.7	17.2	26.0
Mackenzie River basin												
GFDL-ESM2M	9.2	15.1	4.2	3.9	7	10.9	2	5.8	5.3	4.9	8.7	7.5
HadGEM2-ES	7.4	8.5	11.8	7.3	8.2	9.5	8.2	6.2	9.4	4.9	6.1	8.3
IPSL-CM5A-LR	0.1	2.5	2.8	0.6	−0.1	−3.2	0.9	−0.7	−4.4	1.9	−0.7	−6.6
MIROC-ESM-CHEM	8.4	16.2	16.2	8.7	13.9	23.6	9.6	18.6	22.9	7.7	22.1	35.4
NorESM1-M	5.9	9.8	3.5	7.7	5.8	9.5	4.9	7.6	4.6	5.3	6.1	13.5
Mean	6.2	10.4	7.7	5.6	6.9	10.1	5.1	7.5	7.6	4.9	8.4	11.6
HYPE-based projections												
Lena River basin												
GFDL-ESM2M	9.4	8.3	15.4	7.7	13.1	17.8	6.7	9.9	17.4	9.1	14.1	27.4
HadGEM2-ES	5.7	16.2	12.4	7.4	19.3	27.2	5.4	16.1	27.8	12.6	20.8	45.6
IPSL-CM5A-LR	13.2	14.8	18.8	15.3	21.4	22.3	12.8	15.8	26.2	12.1	26.2	47.8
MIROC-ESM-CHEM	7.3	18.8	16.8	3.7	19.4	24.7	4.3	19.5	30.3	9.2	26.7	47.4
NorESM1-M	3.1	7.0	11.3	6.9	9.2	21.3	1.9	4.7	14.8	3.2	13.7	28.9
Mean	7.7	13.0	14.9	8.2	16.5	22.7	6.2	13.2	23.3	9.2	20.3	39.4

Table 2 (continued)

Scenario/GCM	RCP2.6			RCP4.5			RCP6.0			RCP8.5		
	2006–2035	2036–2065	2070–2099	2006–2035	2036–2065	2070–2099	2006–2035	2036–2065	2070–2099	2006–2035	2036–2065	2070–2099
Mackenzie River basin												
GFDL-ESM2M	13.4	20.0	6.0	6.6	9.2	16.6	4.4	12.3	11.1	9.9	14.1	17.3
HadGEM2-ES	10.2	12.0	18.8	9.8	12.1	13.5	12.1	7.6	13.1	6.2	8.5	8.6
IPSL-CM5A-LR	−0.2	4.6	4.5	0.9	1.2	−3.2	−0.3	−3.4	−2.7	4.5	0.9	−7.6
MIROC-ESM-CHEM	8.2	21.8	19.9	8.6	14.9	31.2	8.8	20.4	28.9	5.1	24.3	49.2
NorESM1-M	6.5	12.8	−1.3	10.7	2.5	9.8	5.5	6.5	−0.3	6.1	1.1	16.0
Mean	7.6	14.2	9.6	7.3	8.0	13.6	6.1	8.7	10.0	6.4	9.8	16.7

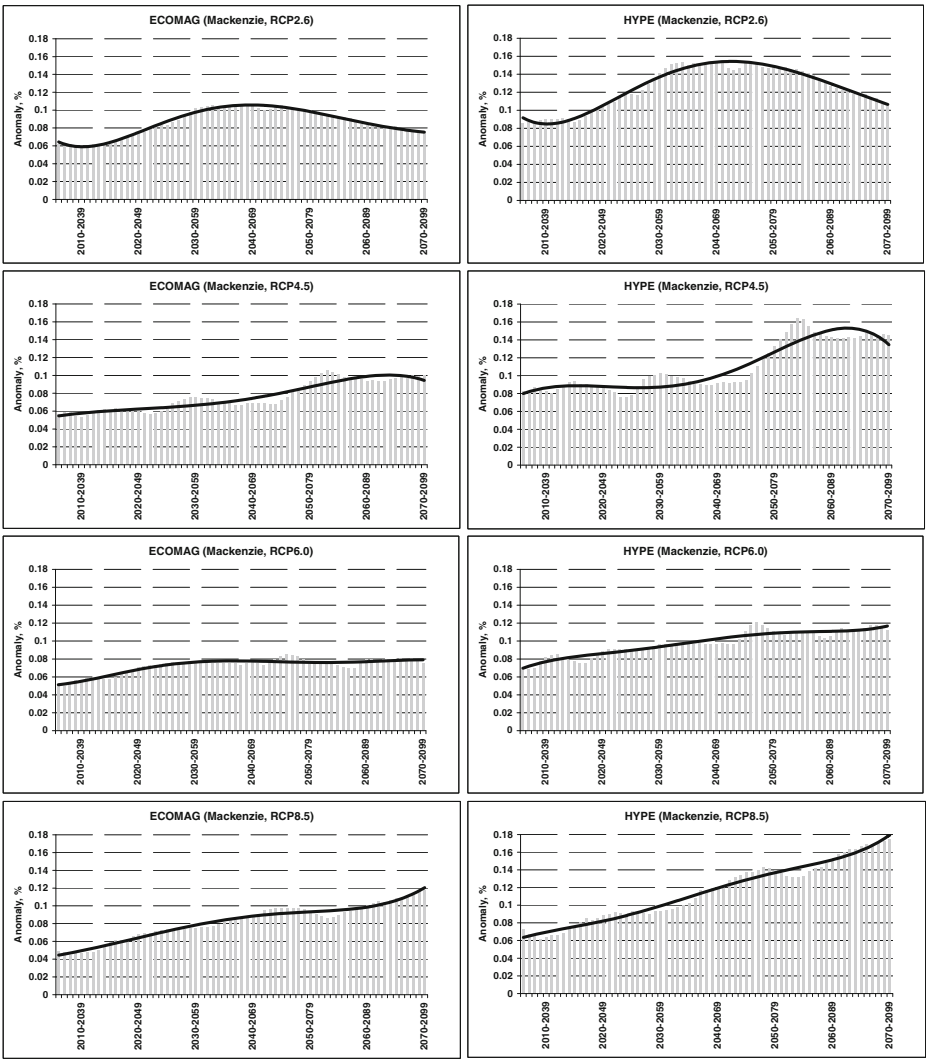

Fig. 1 Moving averaged time series of the mean annual runoff anomaly (*columns*) simulated for the Mackenzie River under the different RCP scenarios (*line* is the polynomial trend). The annual runoff anomaly is calculated by averaging over the anomalies modeled under the outputs of five GCMs for the specific RCP scenario (see Sect. 4.2 for details)

supplementary material present the basin-averaged precipitation and air temperature trajectories calculated by the same smoothing procedure as that used for calculating the runoff trajectories. One can see from Figs. B and C that the precipitation trajectories taken under the same RCP scenario have patterns quite similar to the runoff trajectories shown in Figs. 1 and 2. In other words, the detected delay in the hydrological response to changes in the RCP2.6 scenario is caused by the corresponding delay in precipitation response to these forcing changes. In general, one can conclude that the great basins' water regime shows a multi-year delay in its response to changes in the mitigation RCP scenario and, consequently, also could show a similar delay in response to adaptation measures aiming in limitation of global warming.

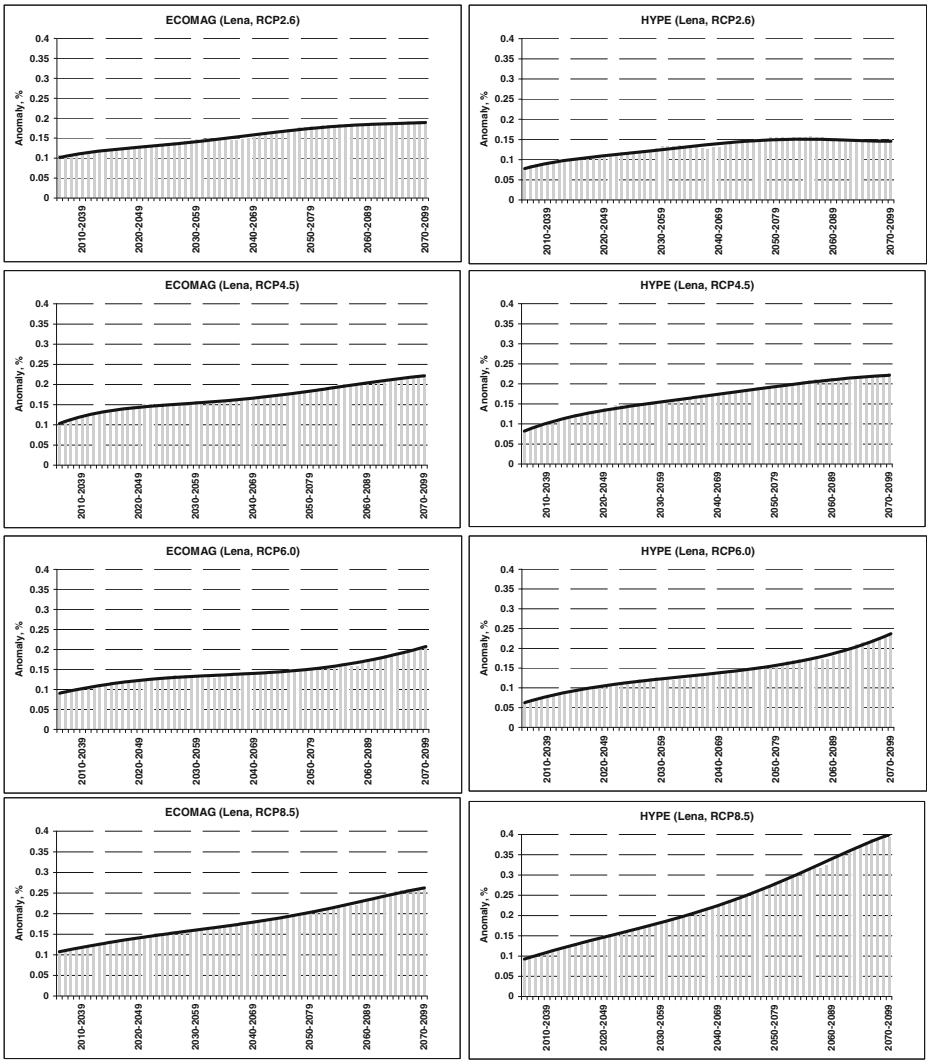

Fig. 2 Moving averaged time series of the mean annual runoff anomaly (*columns*) simulated for the Lena River under the different RCP scenarios (*line* is the polynomial trend) The annual runoff anomaly is calculated by averaging over the anomalies modeled under the outputs of five GCMs for the specific RCP scenario (see Sect. 4.2 for details)

As it was pointed out above (see Sect. 4.3), we analyzed the MAR anomalies and the MMR anomalies to assess contribution of the model (GCM) and scenario (RCP) uncertainties into the variability of the runoff projections. Figure 3 demonstrates variability of the projected MAR anomalies calculated for each 30-year period as described in Sect. 4.3. For both basins, the ECOMAG- and HYPE-derived MAR anomalies turned out to be almost similar but the variability of the HYPE-based estimates is larger. As expected, the variability rises with the time horizon of the projection, and generally, the variability is larger for the Mackenzie than for the Lena basin. The latter can be explained, partly, by the larger precipitation variability in climate projections for the Mackenzie basin compared to the Lena basin.

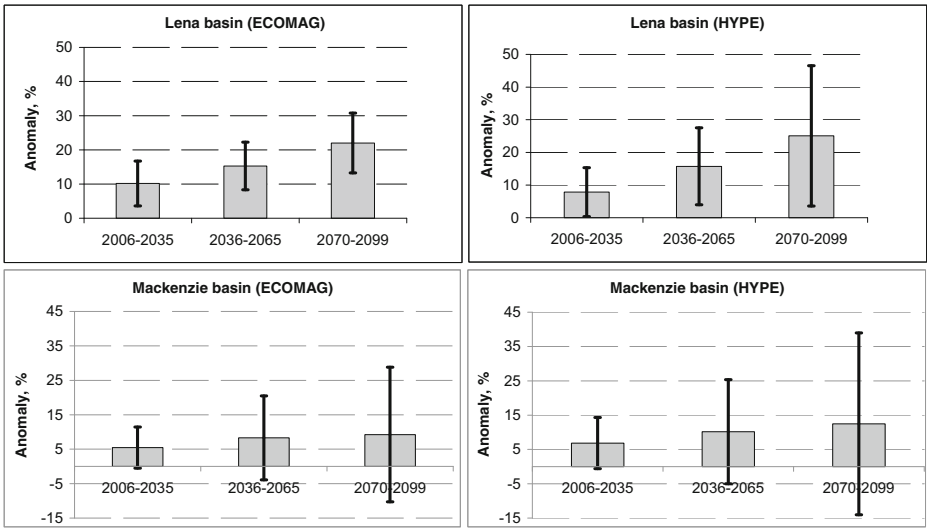

Fig. 3 The projected long-term mean annual runoff anomalies (*gray bars*) and their variability (*vertical lines*) caused by the GCM and the RCP scenario uncertainties (*vertical lines* span the interval $M \pm 1.96$ SD, where M is the mean and SD is the standard deviation of the anomalies)

The MMR anomalies (see Sect. 4.3) and their variability are shown in Fig. 4 for the 2070–2099 period only. For both basins, the largest MMR anomalies were projected for spring months. Reasonable explanation is that large projected growth of monthly temperatures in the cold April–May season (12–14 °C for Lena and 8–10 °C for Mackenie) lead to an increase of seasonal runoff and advancing of snowmelt season from June to May.

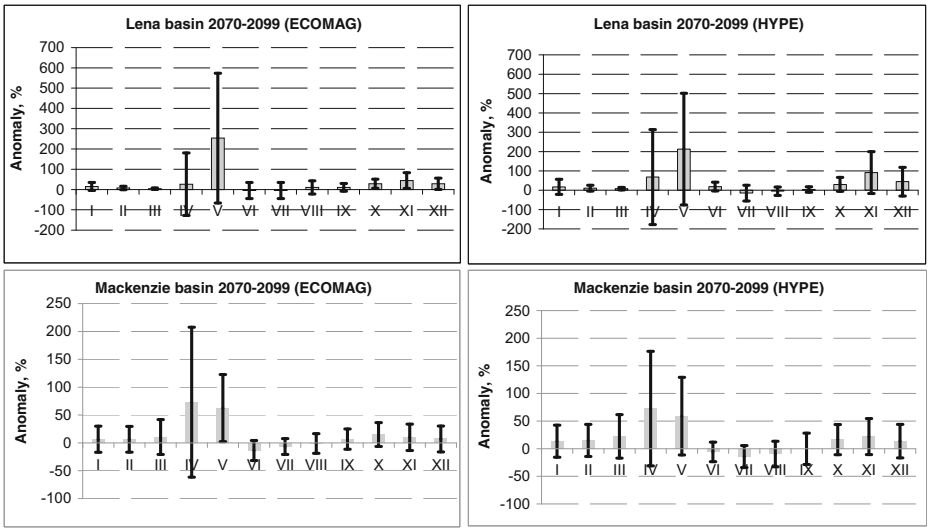

Fig. 4 The projected long-term mean monthly runoff anomalies for 2070–2099 (*gray bars*) and their variability (*vertical lines*) caused by the GCM and the RCP scenario uncertainties (*vertical lines* span the interval $M \pm 1.96$ SD, where M is the mean and SD is the standard deviation of the anomalies)

5.3 GCM-based and MOC-based projections: a comparison

For each 30-year period, 20 (5 GCMs × 4 RCPs) mean annual runoff anomalies simulated by the ECOMAG model forced by GCM data were compared with 20 anomalies simulated under the delta-changed historical data. As pointed out in Sect. 4.4, the changes were assigned in such a way to equate the long-term mean values of the historical climatic data (precipitation, air temperature, and air humidity) to the corresponding values of GCM-projected climatic data. Figure 5a–f shows interrelation between the compared anomalies.

One can see from Fig. 5a–c that the Pearson's correlation coefficient R is rather high in the near-future period, decreases in the next period, and become insignificant in the end-century. Also, there is a bias between the MOC-based and the GCM-based anomalies; in average, the latter are 8–10 % larger than the former. The obtained bias can be explained by the fact that the difference between the GCM-based projected and the historical series of climate parameters is not

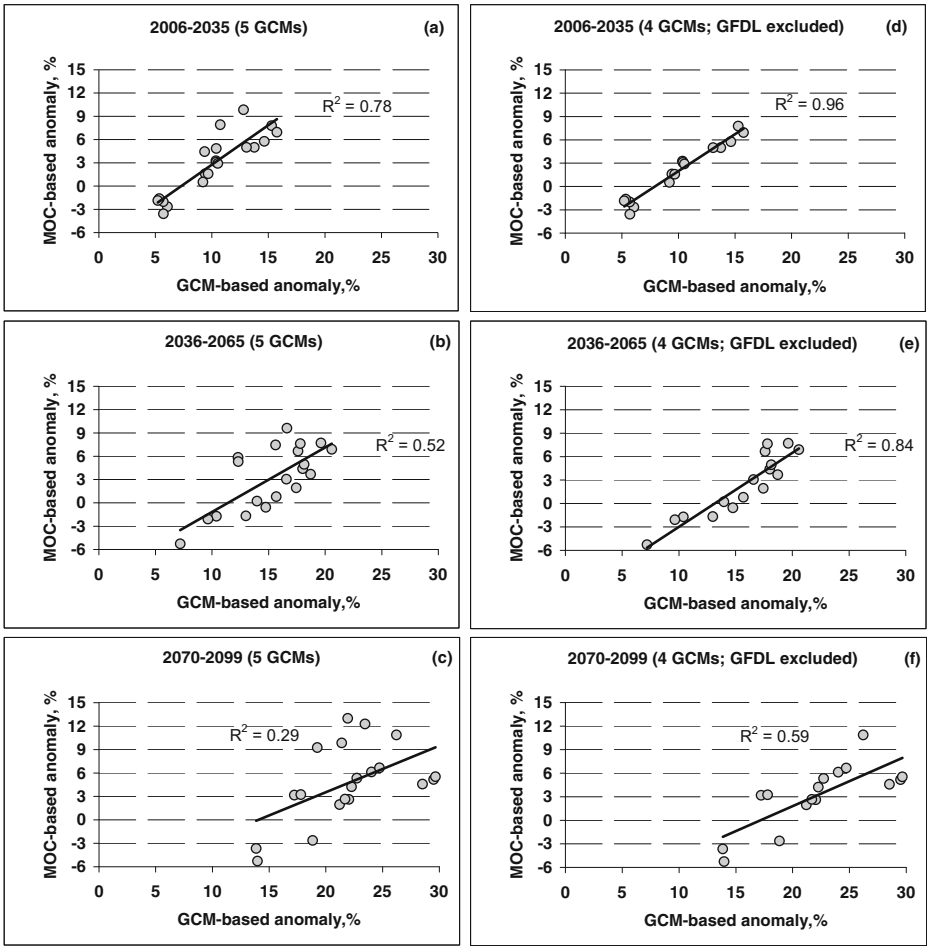

Fig. 5 MOC-based vs. GCM-based projections of the long-term mean annual runoff anomalies (Lena River). **a–c** Twenty (five GCMs × four RCPs) anomalies are used for each plot. **d–f** Sixteen (four GCMs × four RCPs) anomalies are used for each plot (GFDL-ESM2M-based results are excluded)

uniform during a year. Changes in seasonal regime of the climate parameters are also projected (see Fig. D in the supplementary material) and result in the detected bias in hydrological response.

Further analysis shows that excluding four anomalies obtained under one specific GCM (namely, GFDL-ESM2M) leads to a significant improvement of the correlation (Fig. 5d–f) for these periods. This improvement can be explained by differences between the GFDL-ESM2M-projected anomalies of the climate parameters and the anomalies projected by other four GCMs. Fig. D (see supplementary material) demonstrates these differences for monthly anomalies of the air temperature and air humidity deficit for the assigned 30-year periods. In the Lena basin, the main fraction of the annual runoff is generated as a result of snowmelt and melting of ice within an active soil layer during the late-spring and summer seasons. Just for these seasons, the GFDL-ESM2M model gives the air temperature and air humidity monthly anomalies, which are significantly smaller than the anomalies simulated by other four GCMs. These differences in the forcing parameters can be a reason for the obtained discrepant response of hydrological system to the GFDL-ESM2M-based outputs.

It is seen from Fig. 5d–f that for the early-century, the coefficient of determination R^2 between the MOC-based and the GCM-based projections of runoff anomalies when GFDL forcing is excluded is about 0.96 (Fig. 5d). The correlation slightly decreases to $R^2 = 0.84$ (Fig. 5e) by the mid-century and to $R^2 = 0.59$ (Fig. 5f) by the end-century. It is reasonable to assume that the correlation is higher in the beginning of the century, because in this period, the GCM-based series are closer to the delta-changed observed climate in terms of the statistical properties of these series (not only mean values). At the same time, in the mid- and especially in the end-century, the statistical properties of the GCM data may increasingly differ from those of the historical data, and hence, the MOC-based and the GCM-based projections of runoff anomalies are becoming less and less correlated to each other.

6 Conclusion

The main findings of our research can be summarized as follows:

1. Being calibrated and validated under the WATCH forcing climate data during the historical period (1971–2001), both the ECOMAG and the HYPE regional hydrological models driven by the bias-corrected GCM-output data can provide adequate (mean PBIAS of daily discharge lies within [1, 11 %]; mean NSE lies within [0.58, 0.70]) historical runs of the long-term runoff regime for the Lena and Mackenzie basins to be used as references for the GCM-based projections of future climate impacts.
2. Basically, positive mean annual runoff anomalies are projected by the GCM-forced hydrological models for both rivers, independently of future RCP scenario. For the Mackenzie basin, mid- and end-century runoff anomalies derived from the HYPE are several percent larger compared to the ECOMAG anomalies. For the Lena basin, otherwise, the ECOMAG-projected anomalies are larger for the early-century period.
3. The future hydrological projections simulated under the different GCM-based climate scenarios react with a multi-year delay to the assigned changes in the “mitigation” RCP 2.6 scenario. For instance, positive runoff anomalies projected for the Mackenzie under the RCP 2.6 scenario have the same peak-and-decline trajectory as the forcing radiative trajectory but the runoff anomaly peak is projected one to two decades later. The positive runoff anomalies projected for the Lena under the same RCP 2.6 scenario do not decline but

stabilize by the last quarter of the century. The detected delay in the hydrological response to changes in the RCP 2.6 scenario can be explained by the corresponding delay in precipitation response to these radiative forcing changes. This conclusion can be useful for planning the adaptation measures aimed to the limitation of impacts due to global warming.

4. The annual and monthly runoff projections' variability caused by the driving climate models and scenarios rises with the time horizon of the projection. The variability is larger for the Mackenzie than for the Lena (probably, due to the larger precipitation variability in the climate projections for the Mackenzie basin). For both basins, the largest and the most uncertain monthly anomalies were projected for spring months, because large (12–14 °C for Lena and 8–10 °C for Mackenie) projected increase of monthly temperatures in the cold March–May season lead to an increase of seasonal runoff and advancing of snowmelt season from June to May.
5. The modified observed climatology can give, at least for the early-century, useful information on possible runoff changes without the time-consuming experiments with GCMs. For the Lena basin, we found that the mean annual runoff anomalies simulated under the delta-changed historical time series are (when GFDL forcing is excluded) very closely correlated ($R^2 = 0.96$) with the corresponding runoff anomalies simulated under the GCM-based climate projections for the early-century and the correlation decreases to $R^2 = 0.59$ by the end-century. We assume that the correlation is higher in the beginning of the century, because in this period, the GCM-based series are closer to the changed historical series in terms of the statistical properties of these series.

Acknowledgments The authors are very grateful to Guest Editor (Dr. Krysanova) and three anonymous reviewers for their critical and constructive comments. Also, we would like to thank Dr. Pechlivanidis for his valuable suggestions concerning the earliest draft and all ISI-MIP2 project partners who contributed to this study. The presented research of the ECOMAG-team related to the Lena River hydrological modeling was financially supported by the Russian Science Foundation (grant no. 14-17-00700). Part of the ECOMAG team research related to the Mackenzie River hydrological modeling was financially supported by the Russian Ministry of Education and Science (grant no. 14.B25.31.0026). The HYPE modeling was based on the Arctic-HYPE, which is developed within the WMO collaboration of Arctic-HYCOS. Results of the entire Arctic are presented at http://hypeweb.smhi.se. We would like to recognize the initial work done by Kristina Isberg and Dr. Yeshewa Hundecha at SMHI to facilitate the present study.

The present work was carried out within the framework of the Panta Rhei Research Initiative of the International Association of Hydrological Sciences (IAHS).

References

Arheimer B, Dahné J, Donnelly C (2012) Climate change impact on riverine nutrient load and land-based remedial measures of the Baltic Sea Action Plan. Ambio 41:600–612

Aziz OIA, Burn DH (2006) Trends and variability in the hydrological regime of the Mackenzie River basin. J Hydrol 319:282–294

Bartholomé E, Belward A (2005) GLC2000: a new approach to global land cover mapping from Earth observation data. Int J Remote Sens 26(9):1959–1977

Berezovskaya S, Yang D, Hinzman L (2005) Long-term annual water balance analysis of the Lena River. Glob Planet Chang 48(1–3):84–95

Chiew FHS et al (2009) Estimating climate change impact on runoff across southeast Australia: method, results, and implications of the modelling method. Water Resour Res 45(W10414):2009. doi:10.1029/2008WR007338

Donnelly C, Andersson JCM, Arheimer B (2015) Using flow signatures and catchment similarities to evaluate a multi-basin model (E-HYPE) across Europe. Hydrol Sci J. doi:10.1080/02626667.2015.1027710

Ehret U et al (2014) Advancing catchment hydrology to deal with predictions under change. Hydrol Earth Syst Sci 18:649–671. doi:10.5194/hess-18-649-2014

Fischer G et al. (2008) Global agro-ecological zones assessment for agriculture (GAEZ 2008) IIASA, Laxenburg, Austria and FAO, Rome, Italy

Flato G et al. (2013) Evaluation of climate models. In: Climate Change 2013: The Physical Science Basis. Contribution of Working Group I to the Fifth Assessment Report of the Intergovernmental Panel on Climate Change [Stocker TF et al. (eds.)]. Cambridge University Press, Cambridge, United Kingdom and New York, NY, USA

Gelfan A et al (2015a) Large-basin hydrological response to climate model outputs: uncertainty caused by internal atmospheric variability. Hydrol Earth Syst Sci 19:2737–2754. doi:10.5194/hess-19-2737-2015

Gelfan A et al (2015b) Testing the robustness of the physically-based ECOMAG model with respect to changing conditions. Hydrol Sci J 60:1266–1285. doi:10.1080/02626667.2014.935780

Hawkins E, Sutton R (2009) The potential to narrow uncertainty in regional climate predictions. Bull Am Meteorol Soc 90:1095. doi:10.1175/2009BAMS2607.1

Huang S et al. (2016) Evaluation of an ensemble of regional hydrological models in 12 large-scale river basins worldwide. Climatic Change, this issue

Knutti R (2010) The end of model democracy? Clim Chang 102:395–404. doi:10.1007/s10584-010-9800-2

Kundzewicz ZW, Stakhiv EZ (2010) Are climate models "ready for prime time" in water resources management applications, or is more research needed? Hydrol Sci J 55(7):1085–1089

Lindström G et al (2010) Development and test of the ARCTIC-HYPE (Hydrological Predictions for the Environment) model—a water quality model for different spatial scales. Hydrol Res 41(3–4):295–319

Mokhov II, Semenov VA, Khon VC (2003) Estimates of possible regional hydrologic regime changes in the 21st century based on global climate models. Izv Atmos Oceanic Phys 39(2):130

Motovilov Y et al (1999) Validation of a distributed hydrological model against spatial observation. Agric For Meteorol 98–99:257–277

Nijssen B et al (2001) Hydrologic sensitivity of global rivers to climate change. Clim Chang 50:143–175

Nohara D et al. (2006) Impact of climate change on river discharge projected by multimodel ensemble. J Hydrometeor 7:1076–1089. doi:http://dx.doi.org/10.1175/JHM531.1

Pechlivanidis IG, Arheimer B (2015) Large-scale hydrological modelling by using modified PUB recommendations: the India-HYPE case. Hydrol Earth Syst Sci 19:4559–4579. doi:10.5194/hess-19-4559-2015

Pechlivanidis IG et al (2011) Catchment scale hydrological modeling: a review of model types, calibration approaches and the uncertainty analysis methods in the context of recent developments in technology and applications. Glob NEST J 13(3):193–214

Peel MC, Blöschl G (2011) Hydrological modelling in a changing world. Prog Phys Geogr 35:249–261. doi:10.1177/0309133311402550

Seiller G, Anctil F (2014) Climate change impacts on the hydrologic regime of a Canadian river: comparing uncertainties arising from climate natural variability and lumped hydrological model structures. Hydrol Earth Syst Sci 18:2033–2047. doi:10.5194/hess-18-2033-2014

Shiklomanov AI et al (2006) Cold region river discharge uncertainty estimates from large Russian rivers. J Hydrol 326:231–256

Teutschbein C, Wetterhall F, Seibert J (2011) Evaluation of different downscaling techniques for hydrological climate-change impact studies at the catchment scale. Clim Dynam 37:2087–2105. doi:10.1007/s00382-010-0979-8

van Vuuren DP et al (2011) The representative concentration pathways: an overview. Clim Chang 109:5–31. doi:10.1007/s10584-011-0148-z

Woo MK et al. (2008) The Mackenzie GEWEX Study: a contribution to cold region atmospheric and hydrologic sciences. In: Woo MK (Ed.), Cold Region Atmospheric and Hydrologic Studies, the Mackenzie GEWEX Experience, Atmospheric Dynamics 1:1–22.

Xu C, Widen E, Hallding S (2005) Modelling hydrological consequences of climate change—progress and challenges. Adv Atmos Sci 22(6):789–797

Yang D et al (2002) Siberian Lena River hydrologic regime and recent change. J Geophys Res 107(D23):4694. doi:10.1029/2002JD002542

Yang D, Shi X, Marsh P (2015) Variability and extreme of Mackenzie River daily discharge during 1973–2011. Quat Int 380–381:159–168

Ye B, Yang D, Kane DL (2003) Changes in Lena River streamflow hydrology: human impacts vs. natural variations. Water Resour Res 39(7):1200. doi:10.1029/2003WR0011991

Yip QKY et al (2012) Climate impacts on hydrological variables in the Mackenzie River basin. Can Water Resour J 37(3):209